

Extended long range plasmon waves in finite thickness metal film and layered dielectric materials

Junpeng Guo and Ronen Adato

Department of Electrical and Computer Engineering
University of Alabama in Huntsville
Huntsville, AL 35899

jguo@ece.uah.edu

Abstract: In this paper, we show that the propagation distance of the long range plasmon wave mode guided by a finite thickness gold metal film can be extended several orders of magnitude longer if we place intermediate dielectric layers on both sides of the metal film and choose the layer thickness properly. The propagation distance goes to infinite if the intermediate layer thickness approaches a critical thickness.

© 2006 Optical Society of America

OCIS codes: (240.6680) Surface plasmons; (130.2790) Guided waves

References and links

1. H. Raether, *Surface Plasmons on Smooth and Rough Surfaces and on Gratings* (Springer-Verlag, Berlin Heidelberg, 1988).
2. E. N. Economou, "Surface plasmons in thin films," *Phys. Rev.* **182**, 539-554 (1969).
3. J. J. Burke, G. I. Stegeman, and T. Tamir, "Surface-polariton-like waves guided by thin, lossy metal films," *Phys. Rev. B* **33**, 5186-5201 (1986).
4. D. Sarid, "Long-range surface-plasma waves on very thin metal films," *Phys. Rev. Lett.* **47**, 1927-1930 (1981).
5. P. Berini, "Plasmon-polariton waves guided by thin lossy metal films of finite width: Bound modes of symmetric structures," *Phys. Rev. B* **61**, 10484-10503 (2000).
6. P. Berini, "Plasmon-polariton waves guided by thin lossy metal films of finite width: Bound modes of symmetric structures," *Phys. Rev. B* **63**, 125417 (2001).
7. P. Berini, R. Charbonneau, N. Lahoud, and G. Mattiussi, "Characterization of long-range surface-plasmon-polariton waveguides," *J. Appl. Phys.* **98**, 043109 (2005).
8. S. J. Al-Bader, "Optical transmission on metallic wires - fundamental modes," *IEEE J. Quantum Electron.* **40**, 325-329 (2004).
9. B. Lamprecht, J.R. Krenn, G. Schider, H. Ditlbacher, M. Salerno, N. Felidj, A. Leitner, and F.R. Aussenegg, "Surface plasmon propagation in microscale metal stripes," *Appl. Phys. Lett.* **79**, 51-53 (2001).
10. A. Degiron and D. Smith, "Numerical simulations of long-range plasmons," *Opt. Express* **14**, 1611-1625 (2006), <http://www.opticsinfobase.org/abstract.cfm?URI=oe-14-4-1611>.
11. R. Charbonneau, P. Berini, E. Berolo, and E. Lisicka-Shrzek, "Experimental observation of plasmon polariton waves supported by a thin metal film of finite width," *Opt. Lett.* **25**, 844-846 (2000).
12. R. Charbonneau, N. Lahoud, G. Mattiussi, and P. Berini, "Demonstration of integrated optics elements based on long-ranging surface plasmon polaritons," *Opt. Express* **13**, 977-984 (2005).
13. K. Leosson, T. Nikolajsen, A. Boltasseva, and S. I. Bozhevolnyi, "Long-range surface plasmon polariton nanowire waveguides for device applications," *Opt. Express* **14**, 314-319 (2006).
14. L. Holland, *Vacuum Deposition of Thin Films* (Chapman and Hall, London, 1966).
15. G. I. Stegeman and J. J. Burke, "Long-range surface plasmons in electrode structures," *Appl. Phys. Lett.* **43**, 221-223, (1983).
16. F. Y. Kou and T. Tamir, "Range extension of surface plasmons by dielectric layers," *Opt. Lett.* **12**, 367- (1987).
17. L. Wendler and R. Haupt, "Long-range surface plasmon-polaritons in asymmetric layer structures," *J. Appl. Phys.* **59**, pp. 3289-3291 (1986).
18. J. Xia, A. K. Jordan, and J. A. Kong, "Electromagnetic inverse-scattering theory for inhomogeneous

- dielectrics: the local reflection model," J. Opt. Soc. Am. A, **9**, 740-748 (1992).
19. E. Anemogiannis, E. N Glytsis, and T. K Gaylord, "Determination of guided and leaky modes in lossless and lossy planar multilayer optical waveguides: reflection pole method and wavevector density method," J. Lightwave Technol. **17**, 929-941 (1999).
 20. A. Papoulis, *Circuits and Systems* (Holt, Rinehart and Winston, Inc., New York, 1980).
 21. P. B. Johnson and R. W. Christy, "Optical Constants of the Noble Metals," Phys. Rev. B **6**, 4370-4379 (1972).
 22. G. I. Stegeman, J. J. Burke, and D. G. Hall, "Surface-polariton like waves guided by thin, lossy metal films," Opt. Lett. **8**, 383-386 (1983).
 23. J. J. Burke, G. I. Stegeman, and T. Tamir, "Surface-polariton-like waves guided by thin, lossy metal films," Phys. Rev. B **33**, 5186-5201 (1986).
 24. J. A. Dionne, L. A. Sweatlock, H. A. Atwater, and A. Polman "Planar metal plasmon waveguides: frequency-dependent dispersion, propagation, localization, and loss beyond the free electron model," Phys. Rev. B **72**, 075405 (2005).
-

1. Introduction

A surface plasmon wave is the propagation of the free electron density oscillation on the surface of a metal in contact with a dielectric medium. The propagation of the free electron density oscillation creates a localized electromagnetic wave. Surface plasmon waves can only be supported along the boundary of two optical materials with opposite signs of the real parts of the dielectric constants, such as a dielectric and a metal [1, 2, 3]. Surface plasmon waves attenuate rapidly during the propagation due to the intrinsic electron oscillation damping loss in the metal.

A thin metal film embedded in a homogeneous dielectric medium with a symmetric structure supports two guided plasmon wave modes. One mode, which has the symmetric field profile with respect to the center of the metal layer, is called the symmetric mode. Another mode, which has the anti-symmetric field profile with respect to the center of the metal layer, is called the anti-symmetric mode. The symmetric mode has a relatively long propagation distance compared with the surface plasmon wave along the surface of the bulk metal in a dielectric medium. This symmetric surface plasmon wave mode is also called the long range surface plasmon (LRSP) mode. The anti-symmetric mode has a zero in the center of the metal layer and attenuates rapidly during propagation. The anti-symmetric mode is also called the short range surface plasmon mode.

Long range surface plasmon waves have been studied by many authors [4, 5, 6, 7, 8, 9, 10, 11, 12, 13]. The fundamental reasons that thin metal films (or strips) in symmetric structures can support long range plasmon waves are: (1) most energy is located in the surrounding dielectric material for thin metal films; (2) the surface plasmon waves associated with two boundaries travel with the same velocity due to the symmetry of the guide structure.

Although long range plasmon wave modes can be supported by thin metal films in homogeneous dielectric media with symmetric structures, the long range modes still attenuate due to the electron oscillation damping loss in the metal. To increase the travel distance of the long range plasmon mode, a simple strategy is to reduce the metal layer thickness. But it is experimentally difficult to deposit homogeneous metal film of less than 15 nm thickness because metals, such as gold (Au), typically form nanoscale islands in the initial deposition process [14].

Surface plasmon waves guided by multiple parallel thin metal films placed closely together have been studied [15]. Range extension of plasmon waves has been studied with multiple dielectric layers in asymmetric waveguide structures [16]. The extended long range modes in [16] were leaky modes. Long range modes of thin metal films between two different semi-infinite uniform dielectric materials have been studied in [17]. The extended long range modes in the asymmetric waveguides were also leaky modes. In this work, we studied the guided plasmon wave modes along a finite thickness thin metal (Au) film in inhomogeneous layered dielectric materials with symmetric waveguide structures. We found that if we place

intermediate dielectric layers with different dielectric constant on both sides of the metal film, the propagation distance of the symmetric long range mode can be extended several orders of magnitude. Also we found that when the intermediate dielectric layer thickness approaches certain critical thickness, the propagation distance of one long range goes to infinite.

2. The reflection pole method

The plasmon waveguide structure we studied is shown in the Fig. 1. Fig. 1 is the cross section of a thin metal film in inhomogeneous layered dielectric materials. A semi-infinite dielectric medium (ϵ_0) is in the bottom. A thin metal film (Au) layer ($\epsilon_2 = \epsilon_m$) of thickness d_2 is in the middle. One intermediate dielectric layer (ϵ_1) of thickness d_1 is place between the metal layer and the dielectric medium in the bottom cladding. Another intermediate dielectric layer (ϵ_3) of thickness d_2 is place between the metal layer and the dielectric medium in the top cladding. Another semi-infinite dielectric medium (ϵ_4) is on the top of the top intermediate dielectric layer. The two intermediate dielectric layers have the same dielectric constant ($\epsilon_1 = \epsilon_3$) and the same thickness ($d_1 = d_3$). The top dielectric cladding is the same material as the bottom dielectric cladding ($\epsilon_0 = \epsilon_4$). Therefore, the plasmon waveguide structure is symmetrical with respect to the center of the metal layer.

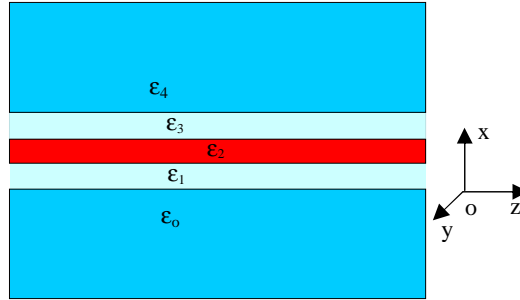


Fig. 1. The plasmon waveguide structure of a thin metal film in layered inhomogeneous dielectric materials.

We are only interested in the guided plasmon modes in this waveguide structure. We use the reflection pole method [18, 19] to calculate the plasmon wave modes. Since the plasmon wave modes are TM mode, we write the magnetic fields in the different regions as

$$H_{yi} = \{A_i \exp[-k_{xi}(x - x_{i-1})] + B_i \exp[k_{xi}(x - x_{i-1})]\} \exp[-j\gamma z], \quad i = 0, 1, 2, 3, 4. \quad (1)$$

In the above equation, $k_{xi} = \sqrt{\gamma^2 - \epsilon_i k_0^2}$ are the x components of complex wave vectors in different regions, γ is the propagation constant (complex) in the z direction. A_i and B_i are coefficients corresponding to the propagating waves in x and $-x$ directions in the i -th region. k_0 is the wave number in the free space.

We assume that an incident transverse magnetic (TM) electromagnetic wave is incident to the boundary of ϵ_0 and ϵ_1 from the bottom of the waveguide structure. At each boundary, the tangential components of the magnetic field H_{yi} and the electrical field $E_{zi} = \frac{1}{j\omega\epsilon_i} \frac{\partial H_{yi}}{\partial x}$

are continuous. By applying these boundary conditions, we have

$$\begin{pmatrix} A_4 \\ B_4 \end{pmatrix} = T_3 T_2 T_1 T_0 \begin{pmatrix} A_0 \\ B_0 \end{pmatrix} = \begin{bmatrix} t_{11} & t_{12} \\ t_{21} & t_{22} \end{bmatrix} \begin{pmatrix} A_0 \\ B_0 \end{pmatrix}, \quad (2)$$

where

$$T_i = \frac{1}{2} \begin{pmatrix} \left[1 + \frac{\varepsilon_{i+1}}{\varepsilon_i} \frac{k_{xi}}{k_{x(i+1)}} \right] \exp(-k_{xi}d_i) & \left[1 - \frac{\varepsilon_{i+1}}{\varepsilon_i} \frac{k_{xi}}{k_{x(i+1)}} \right] \exp(k_{xi}d_i) \\ \left[1 - \frac{\varepsilon_{i+1}}{\varepsilon_i} \frac{k_{xi}}{k_{x(i+1)}} \right] \exp(-k_{xi}d_i) & \left[1 + \frac{\varepsilon_{i+1}}{\varepsilon_i} \frac{k_{xi}}{k_{x(i+1)}} \right] \exp(k_{xi}d_i) \end{pmatrix}, \quad i = 0, 1, 2, 3. \quad (3)$$

The relationship between the incident, the reflection, and the transmission is given in

$$\begin{pmatrix} A_4 \\ 0 \end{pmatrix} = \begin{bmatrix} t_{11} & t_{12} \\ t_{21} & t_{22} \end{bmatrix} \begin{pmatrix} 1 \\ B_0 \end{pmatrix}. \quad (4)$$

The reflection coefficient is

$$R = \frac{B_o}{A_o} = -\frac{t_{21}}{t_{22}}. \quad (5)$$

The reflection coefficient (R) is a function of the complex propagation constant $\gamma = (n - jn_i)k_0$. The guided plasmon modes are the modes which propagate in the z direction and exponentially decay away from the metal layer in the x and $-x$ directions. The guided modes correspond to the resonances of the layered waveguide structure, which happen at the poles of the reflection coefficient R . The poles of the reflection coefficient are the solutions of $t_{22}(\gamma) = 0$.

Finding the roots of the complex equation $t_{22}(\gamma) = 0$ is numerically challenging. Reflection pole method (RPM) monitors the phase of $t_{22}(\gamma)$ as a function of the real part index (n) of the propagation constant. The plasmon wave guided modes correspond to the rapid changes of the phase of t_{22} . According to Bode plot theory [20], a peak of the derivative of the phase of t_{22} corresponds to the real part index of a guided mode, and the full width at the half maximum of the phase derivative curve is the imaginary part of mode index.

Using the reflection pole method, we searched the plasmon wave modes for a gold (Au) metal film of 20 nm thickness embedded in the silicon dioxide dielectric material ($\varepsilon_o = \varepsilon_4 = (1.45)^2$) at the 1.55 micron wavelength ($d_1 = d_3 = 0, d_2 = 20$ nm). The dielectric constant of gold film at 1.55 micron [21] is $\varepsilon_2 = -114.925 - 11.0918j$. Fig. 2 (a) is the plot of the phase of t_{22} versus the real part of the propagation constant index. Fig. 2 (b) is the derivative of the phase of t_{22} versus the real part of the propagation constant index. From the Fig. 2, we see two rapid changes of the phase of t_{22} . These two rapid phase changes correspond to two guided plasmon wave modes. Once we know the approximate values of the mode index from the plot, we can numerically solve the equation $t_{22} = 0$ with the initial guess of its roots.

The complex mode indices we found are $n_1 = 1.45229459 - 0.00003345585j$, $n_2 = 1.525501873 - 0.013489423j$. Both modes are guided modes. The first mode is the symmetric mode (s_b) which has a propagation distance ($1/e$ of the intensity) of 3686.8 micron. The second mode is the anti-symmetric (a_b) mode, which has a propagation distance of 9.144 micron. The mode size (full width at $1/e$ of the maximum intensity) of the symmetric mode is 3.0429 micron. The mode size of the anti-symmetric mode is 0.54047 micron.

The surface plasmon mode properties of thin metal films embedded in infinite homogeneous dielectric materials have been studied by many authors [4, 22, 23, 24] through solving the dispersion equation. To verify the modes obtained with the reflection pole method, we derived the dispersion equation by applying the boundary conditions of the Maxwell

equations and numerically search the roots of the dispersion equation. We found two solutions: $1.452293989-0.00000334539j$ and $1.52550212-0.01348915j$. These two solutions agree well with the results obtained by using the reflection pole method. This validates the RPM method.

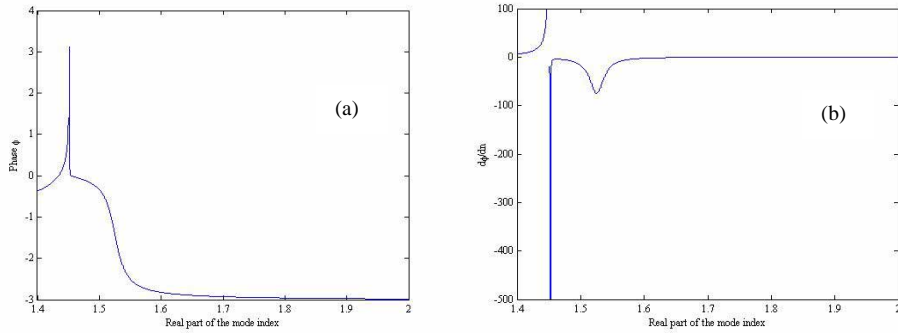


Fig. 2. (a) The phase of t_{22} versus the real part of the mode index; (b) the derivative of the phase of t_{22} versus the real part of the mode index.

3. Higher dielectric constant intermediate layer

First we chose a thin gold (Au) film as the metal layer and silicon nitride ($\epsilon_1 = \epsilon_3 = 4.0$) as the intermediate layer material and silicon dioxide ($\epsilon_0 = \epsilon_4 = (1.45)^2$) as the top and bottom cladding material ($\epsilon_1 = \epsilon_3 > \epsilon_0 = \epsilon_4$). The thickness of the gold metal layer is $d_2 = 20$ nm. For the intermediate dielectric layer thickness (d_1 and d_3) of 1000 nm, we plot the phase (ϕ) of t_{22} as the function of the real part mode index in Fig. 3 (a). We see the stair case phase π changes at certain values of the real part of the mode index.

According to Bode plot theory [20], each π phase change corresponds to the real part of the root of t_{22} . The imaginary part of the root of t_{22} corresponds to the width of the phase derivative curve ($d\phi/dn$) of t_{22} . Fig. 3 (b) shows the phase derivative versus the real part of the mode index. Once we know the approximate values of mode indices from the plot, we numerically solved the equation $t_{22} = 0$ with the initial guesses of its roots. For the intermediate dielectric layer thickness of 1000 nm, we found four complex solutions: $n_1 = 1.732403005 - 0.0001470494j$, $n_2 = 1.80394551 - 0.00522046879j$, $n_3 = 1.989189193 - 0.000206846j$, $n_4 = 2.194229366 - 0.0341893452j$. To verify these solutions are indeed the poles of the reflection coefficient, we input these complex numbers to the t_{22} , and find $|\text{Re}[t_{22}]| < 10^{-21}$ and $|\text{Im}[t_{22}]| < 10^{-21}$. These four solutions are all guided plasmon wave modes.

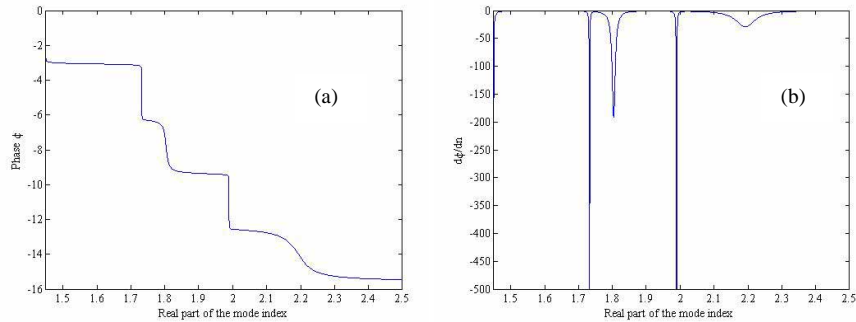


Fig. 3. (a) The phase of t_{22} versus the real part of the mode index; (b) the derivative of the phase of t_{22} versus the real part of the mode index.

The properties of these guided modes are listed in the Table 1. The longest range plasmon wave mode is the mode (a) which has the smallest imaginary part of the mode index. The propagation distance of this mode is 838.8 micron. The propagation distance is defined as the travel distance where the intensity decreases a factor of $1/e$. The mode (c) is the second long range plasmon mode. The propagation distance of the second long range mode is 596.314 micron. The modes (b) and (d) are the two short range modes. The propagation distances of the short range modes are one order of magnitude less than the long range modes.

We plotted the magnetic field mode profiles (H_y) of these four guided plasmon modes in Fig. 4. The modes (c) and (d) are the fundamental modes. The modes (a) and (b) are the higher order modes. We see that the long range modes (a) and (c) are symmetric modes. The short range modes (b) and (d) are anti-symmetric modes. The mode profiles are similar to the profiles of the dielectric waveguide modes, but have significant deviations from the dielectric waveguide modes near the metal layer due to the surface plasmon effect.

Table 1. Guided plasmon wave modes for the intermediate layer thickness of 1000 nm

Mode	Real part of the mode index	Imaginary part of the mode index	Propagation distance (micron)
(a)	1.732403005	0.0001470494	838.80
(b)	1.803945510	0.0052204688	23.627
(c)	1.989189193	0.0002068460	596.314
(d)	2.194229366	0.0341893452	3.6077

Using the same technique, we searched the guided plasmon wave modes for varying intermediate dielectric layer thickness starting from zero to one micron. The gold metal film was fixed at 20 nm. Fig. 5 (a) shows the real part of the mode index of the guided plasmon wave modes for different intermediate layer thickness. We see that the structure supports two guided modes for the intermediate layer thickness less than 465 nm. The third guided mode (dashed green line) starts when the intermediate layer thickness reaches 465 nm. The structure starts to support the fourth guided mode (red dot line) when the intermediate layer thickness reaches 543 nm. As the intermediate dielectric layer thickness continuously increases, we expect that more guided modes will be supported. Fig. 5 (b) shows the imaginary part of the mode index of the four guided plasmon modes for varying intermediate layer thickness.

Figure 6 shows the propagation distances versus the intermediate dielectric layer thickness for these guided plasmon modes. We see that when the intermediate layer thickness is approaching to a critical thickness, the propagation distance of the longest range plasmon mode goes to infinite. For the intermediate layer thickness of 543 nm, the complex mode index of the longest range mode (red dot line) is $1.4500012-7.91467 \times 10^{-7}$. The propagation distance of this mode is 155.844 mm. This propagation distance is approximately 42 times of the propagation distance of the long range plasmon wave mode guided by the gold film of same thickness without intermediate dielectric layers.

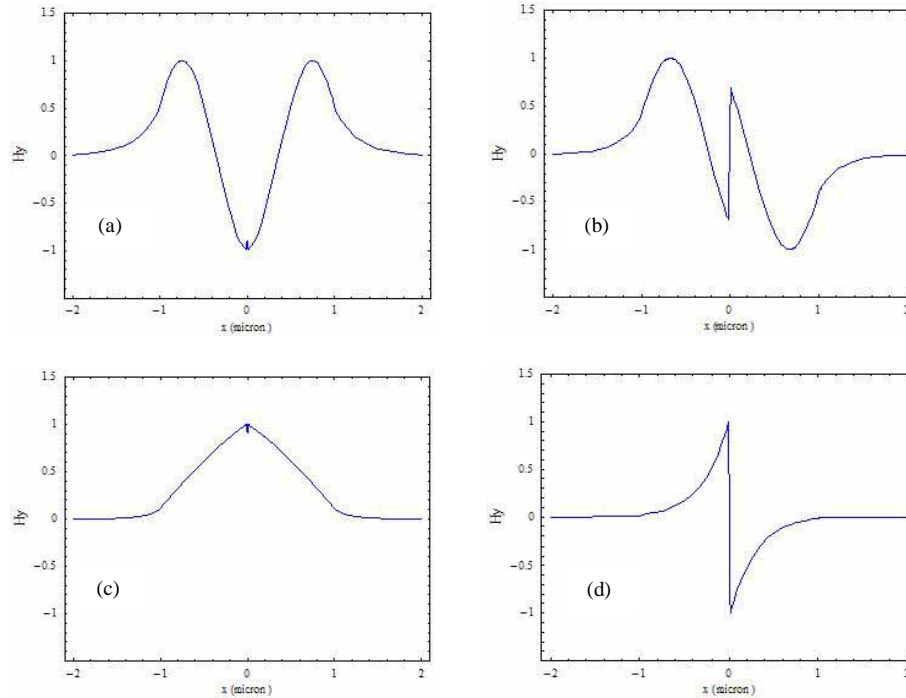


Fig. 4. The magnetic field H_y (in the unit of A/m) profiles of the guided plasmon modes. (a) is the longest range mode; (b) is one short range mode; (c) is the second long range mode; and (d) is the second short range mode.

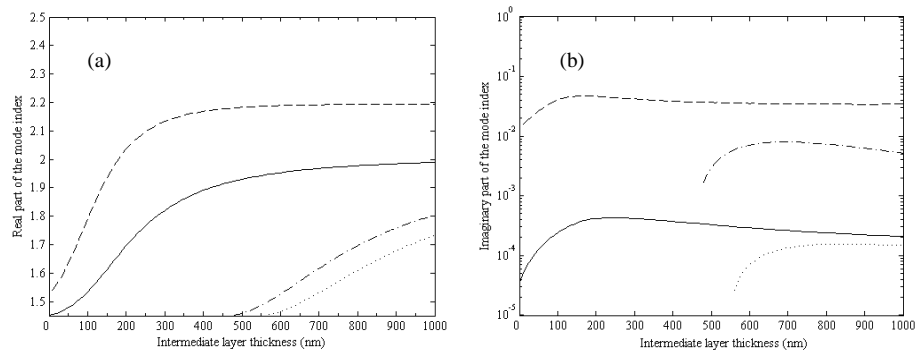


Fig. 5. (a) The real part of the mode index for varying intermediate dielectric layer thickness; (b) the imaginary part of the mode index for varying intermediate dielectric layer thickness.

It is well known that without the metal film, this waveguide structure supports dielectric waveguide modes. Dielectric waveguide modes are due to the total internal reflections from the boundaries of the high and the low index materials. Depending on the thickness of high index material layer and the contrast of the index of refraction, the dielectric waveguide can support only the fundamental symmetric mode with the *Cosine* function mode profile in the high index region or support additional higher order modes with the *Sine* and *Cosine* function mode profiles. With the presence of the metal film, the modes we have found here are due to the two effects: the total internal reflection effect and the surface plasmon effect. The mode profiles shown in Fig. 4 (b), (c), and (d) deviates significantly from the mode profiles of the dielectric waveguide due to the surface plasmon effect. The extended long travel ranges for

the two symmetric modes are because the electromagnetic energies of the guided modes are located mostly in the dielectric media which are assumed as lossless in our calculations.

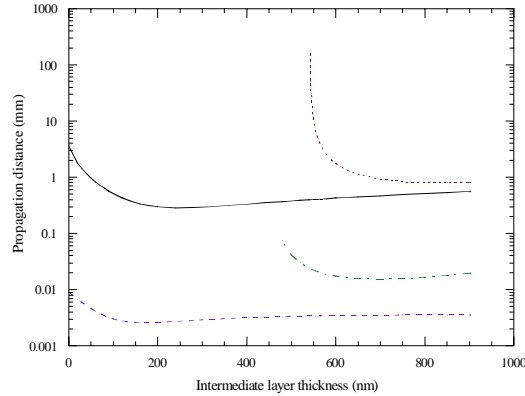


Fig. 6. Propagation distances of the guided modes versus intermediate layer thickness for the gold film thickness of 20 nm.

4. Lower dielectric constant intermediate layer

Then we chose the lower dielectric constant silicon dioxide ($\epsilon_1 = \epsilon_3 = (1.45)^2$ at 1.55 micron) as the intermediate layer dielectric material and the high dielectric constant silicon nitride ($\epsilon_0 = \epsilon_4 = 4.0$ at 1.55 micron) as the top and bottom cladding material ($\epsilon_1 = \epsilon_3 < \epsilon_0 = \epsilon_4$). The thickness of the gold metal layer is kept the same at $d_2 = 20$ nm. We searched the guided plasmon wave modes for different intermediate silicon dioxide dielectric layer thickness. Fig. 7 (a) shows the real part of the mode index for different intermediate dielectric layer thickness. The solid line curve is the real part of the mode index of the long range mode. The dashed line curve is the real part of the mode index of the short range mode. From Fig. 7 (a), we see that two guided modes are supported when the intermediate dielectric layer thickness is smaller than a critical thickness. Fig. 7 (b) shows the imaginary part of the mode index versus the low index intermediate layer thickness for the long range mode (solid line curve) and the short range mode (dashed line curve).

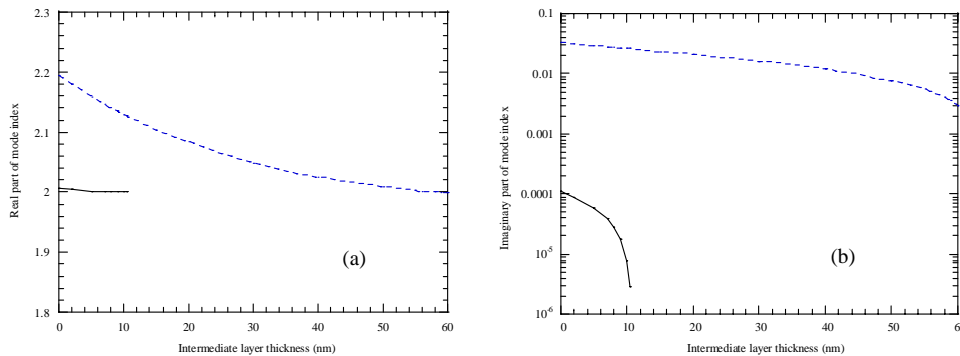


Fig. 7. (a) The real part of the guided mode index versus the intermediate layer thickness; (b) the imaginary part of the guided mode index versus the intermediate layer thickness.

Figure 8 shows the propagation distance versus different intermediate layer thickness for the two guided modes. One mode is the long range mode (solid line curve). Another is the short range mode (dashed line curve). When the intermediate layer approaches to a critical thickness, the propagation distance of the long range mode goes to infinite. The critical intermediate layer thickness is approximately at 10.7 nm. At the intermediate layer thickness

of 10.5 nm, the propagation distance of the symmetric mode is 43.037 mm. This propagation distance is approximately 38 times of the propagation distance of the long range mode without the intermediate layer. The size of the mode is 63.194 micron in the x direction. Beyond the critical thickness, the symmetric mode disappears. When we increase the intermediate layer thickness to about 59 nm, the real part of the effective mode index of the short range mode becomes smaller than the index of refraction of the cladding material. The short range mode becomes a leaky mode and no more guided plasmon wave mode exists.

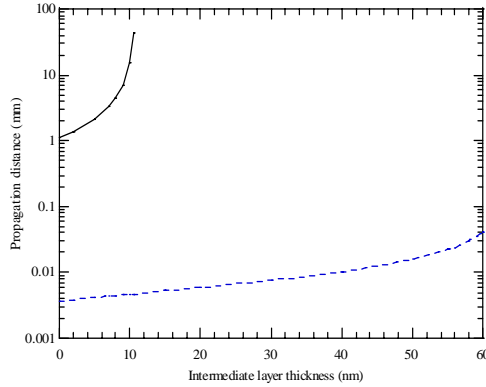


Fig. 8. The propagation distances of the two guided plasmon wave modes versus the intermediate dielectric layer thickness.

We plotted the magnetic field mode profiles (H_y) of two guided plasmon modes for the intermediate layer thickness of 10.5 nm. The long range symmetric mode magnetic field profile is shown in Fig. 9 (a). Fig. 9 (b) is the close look of the mode profile near the metal layer. We see that the symmetric mode has a small notch inside the metal layer. This small notch is due to the electromagnetic field absorption inside the metal material. The short range magnetic field profile is shown in Fig. 10 (a). Fig. 10 (b) is the close look of short range magnetic field profile near the metal region. The anti-symmetric mode magnetic field reaches zero in the center of the metal layer.

Without the metal film, the waveguide structure cannot support any dielectric waveguide mode since the intermediate dielectric layer has the lower index of refraction than the cladding dielectric material. Both the long range mode and the short range mode here are purely due to the surface plasmon effect. The extended ultra-long travel range of the symmetric mode is due to the redistribution of the electromagnetic energy caused by the presence of the low index intermediate layers. More electromagnetic energy propagates in the dielectric media.

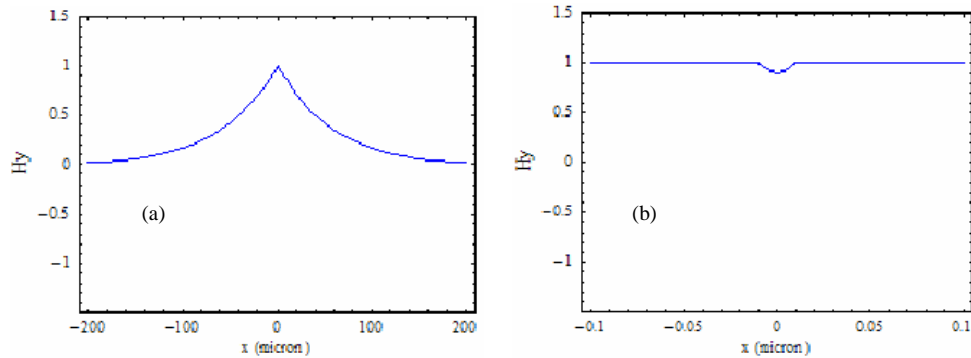


Fig. 9. Magnetic field mode profile (in the unit of A/m) of the long range mode at the intermediate layer thickness $d=10.5$ nm.

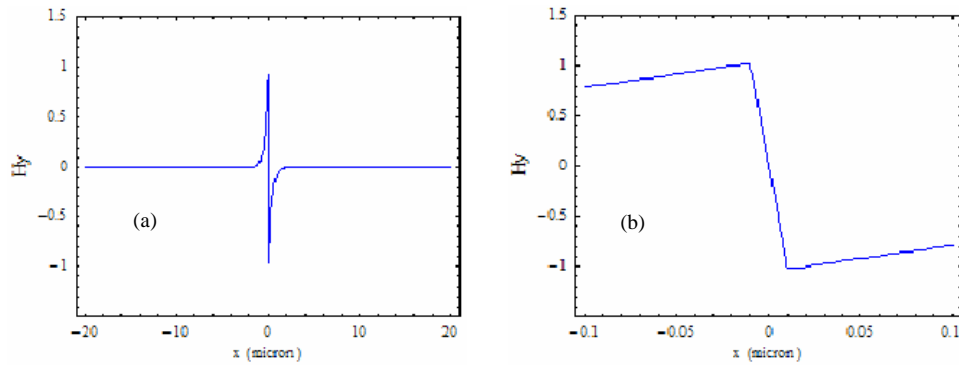


Fig. 10. Magnetic field mode profile (in the unit of A/m) of the short range mode at the intermediate layer thickness of $d=10.5$ nm.

5. Summary

We studied the guided plasmon wave modes of a thin gold metal film in inhomogeneous layered dielectric materials with the reflection pole method. The inhomogeneous layered plasmon waveguide structure consists of a finite thickness gold metal film and two identical dielectric intermediate layers on both sides of the metal film in a homogeneous dielectric material. The intermediate dielectric layers have a different dielectric constant from the surrounding uniform dielectric medium. First, we studied the guided plasmon wave modes by choosing the high dielectric constant material as the intermediate layer material and the low dielectric constant material as the top and bottom homogeneous cladding dielectric material. We found that multiple guided long range modes can be supported by this kind of structure and one of them can propagate sever orders of magnitude longer than the long range mode of the same thickness thin metal film in the homogeneous dielectric medium. As the intermediate layer thickness approaches to a critical thickness, the propagation distance of this long range mode goes to infinite. Without the metal film, this structure supports the dielectric waveguide modes, which are based on the principle of the total internal reflection. With the metal film, the modes we have found here are due to the two effects: the total internal reflection from the dielectric-dielectric boundaries and the surface plasmon oscillation. Then, we studied the guided modes by choosing the low dielectric constant material as the intermediate layer material and the high dielectric constant material as the top and bottom cladding dielectric medium. As we increase the low index intermediate layer thickness from zero, the propagation distance of the symmetric long range plasmon wave mode increases. The travel range of the long range mode goes to infinite when the intermediate layer approaches to a critical thickness. In this later case, the structure without metal film cannot support any guided mode since the intermediate dielectric layer material has the lower index of refraction than the surrounding homogeneous dielectric material. Both the long range mode and the short range mode are purely due to the surface plasmon effect. We believe that this ultra-long range surface plasmon waveguide structure with low index intermediate layers will have many applications since the symmetric mode profile is close to the Gaussian shape, which enables reasonably large couple efficiency from Gaussian beam laser to the plasmon wave mode.

In summary, our studies have shown that the propagation distance of one guided plasmon wave mode of a thin metal film in inhomogeneous layered dielectric materials can be extended several orders of magnitude longer than the long range mode of the metal film of the same thickness in homogeneous dielectric medium. The propagation distance of this very long range mode goes to infinite as the intermediate layer thickness approaches to the critical thickness.